Robotica (1997) volume 15, pp 407–416. Printed in the United Kingdom 

# The 6-Dof 2-Delta parallel robot

J.P. Lallemand, A. Goudali and S. Zeghloul

*Laboratoire de Mécanique des Solides, U.M.R. C.N.R.S 6610, SP2MI-B.P. 179 86960 FUTUROSCOPE Cédex (France)*

**SUMMARY**

In this paper, we will present a new 6-DOF parallel robot using a set of two Delta structures. An effective method is proposed to establish explicit relationships between the end effector co-ordinates and the active and passive joint variables. A simulation of the 2-Delta robot on a C.A.D. Robotics system will also be presented. This simulation will allow us to validate the cohesion of our calculations, and to show the workspace depending on the mechanical limits on passive joints variables. Finally, an approach is proposed to study the influence of small clearances of the passive joint on the precision of the position and rotation of the effector. This approach is based on a concept similar to that of Yoshikawa's manipulability.

KEYWORDS: Parallel robot; Uncoupled; Modelization; Workspace; Ellipsoid of clearance.

## 1. INTRODUCTION

Parallel robots have been the subject of several studies due to the considerable interest they have demonstrated through their lightness, rigidity and rapidity. These particular properties open the door to all spatial applications where mass problems are particularly crucial. They are also used as robot end effector. The first parallel robot structure dates from 1939 when Pollard[1] proposed a parallel structure to paint cars. In 1949, Gough proposed an articulated machine to test tires. Next Stewart[2] suggested the utilisation of this structure as a movement generator for flight simulators. It was also used by Reboulet,[3] and by Merlet[4] as a compliant wrist of a robot. Amongst spatial operators of 3 d.o.f., the Delta structure designed by Clavel[5] constitutes technological innovation. Other 3 d.o.f. parallel structures have been developed. Three of these are the parallel robot H-Star developed by Hervé,[6] the robot Speed R-Man developed by Reboulet[7] and the structure proposed by Jacquet.[8]

We will put forward the 2-Delta robot which in principle, constitutes a new and original structure. This robot is entirely parallel and possesses 6 d.o.f. Its features lie in mechanical uncoupling of translation and orientation motions. This property is what differentiates it from other traditional 6 d.o.f parallel robots or from the one issued from the Delta structure. This paper partially treats the different studies that have been carried out on the 2-Delta robot and which have been presented in reference 9.

## 2. PRINCIPLE OF THE 2-DELTA STRUCTURE

In Figure 1(a) we can see the well known Delta architecture proposed by Clavel. It is a 3 d.o.f. mechanism for which the moving platform remains parallel to the base platform.

It is easy to see that Delta mechanism is equivalent to an open loop kinematic chain composed of 3 orthogonal prismatic joints as shown in Figure 1(b). This observation will be used later.

Starting from Clavel's discovery, many authors have proposed translation devices shown, for example, in Figure 2 and Figure 3. The H-star robot by Herve which allows for a very large displacement in X-direction is depicted in Figure 2. And in Figure 3 the translation device by Jacquet in which the authors put double universal joints in the place of double parallel rods is shown.

Many robotic tasks need the end effector rotates in addition to the 3 d.o.f. in translation. The 4 d.o.f. Delta Robot in which the gripper is connected to the moving platform by a revolute joint and to the actuator by means of telescopic arm is seen in Figure 4. If 6 d.o.f. are needed we will use the Hexa Robot proposed by Pierrot[10] represented in Figure 5.

In the case presented in Figure 4, we notice that the rotation of the end effector does not depend on its translation, which is a good result that does not exist in the Hexa Robot, unfortunately the end effector has only one d.o.f. in rotation.

The problem that we seek to resolve may be formulated in the following way. How to find a mechanism on Delta architecture that would allow us to obtain 3 d.o.f. rotation for the end effector not depending on its translation and actuated by motors fixed on the base of the Delta.

One solution has been studied using the following idea that is illustrated in Figure 6(a).

Here, the gripper is connected to moving platform by a spherical joint $R_n$. An "input rod" is also connected to the fixed base by spherical joint $R_b$. The question is: what kind of links joined together between gripper and "input rod" must we use so that the rotation of the gripper will be independent from the translation of the moving platform. And so, this kinematic chain must allow free translations and forbid rotations between "input rod" and gripper. Such a kinematic chain could be constituted, as shown in Figure 6(b), by a set of 3 links connected together by 3 orthogonal prismatic joints. As it has been mentioned previously, this kinematic chain represents the equivalent open loop kinematic chain for the Delta mechanism shown in Figure 1(b). Therefore, as shown in

https://doi.org/10.1017/S0263574797000507 Published online by Cambridge University Press

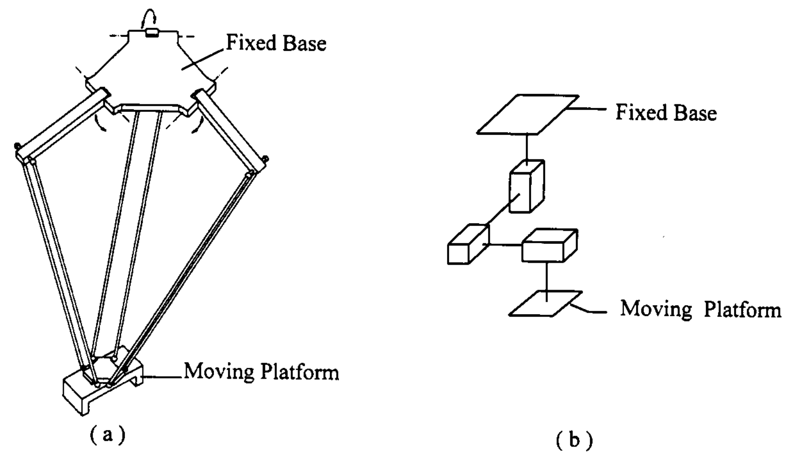


Fig. 1. (a) Three d.o.f. Delta architecture (b) Equivalent open loop kinematic chain.

Figure 7, we can use a Delta mechanism whose moving platform and base platform are rigidly connected to the end effector and to the "input rod", respectively. Thus, we obtain the 6 d.o.f. Delta decoupled parallel robot. The external Delta controls the translation movement of the end effector, whereas the internal Delta controls its rotation movement.

Actually, in order to obtain the rotation movement of the orientable base, we could put a spherical 3 d.o.f. parallel manipulator proposed by Gosselin[11] in the place of the input rod.

In Figure 8 is shown a prototype without actuators of the 2-Delta robot. This device allows us to verify that the rotation and translation motions of the gripper are independent. The device is composed of 21 bodies connected together by 26 spherical joints and 6 revolute joints. Due to the great number of bodies and joints we had to verify that the 2-Delta robot is not an overconstraint mechanism. The device we developed is actually a non-overconstraint mechanism.

## 3. KINEMATICS MODELING OF THE 2-DELTA STRUCTURE

The modelization of parallel robots is quite specific. There is no existing systematic and simple model, therefore it is necessary to find the well adapted methods of each structure. In the case of the 2-Delta robot, we propose an analytic modelization of the direct kinematic problem as well as of the inverse kinematic problem.

### *3.1. Notations and mechanical limits on joints variables*

In Figure 9 we show how to define joint variables. Here, $B_i C_i$ is a virtual rod which represents the double parallel rods. $\theta_1^i$, $\theta_2^i$, $\theta_3^i$, $\beta_2^i$, $\beta_3^i$ are the joint angles for the kinematic chain numbered $i$ for the external Delta, while $\psi_1^i$, $\psi_2^i$, $\psi_3^i$, $\delta_2^i$, $\delta_3^i$ are the joint angles for the kinematic chain numbered $i$ for the internal Delta.

The $\beta_j^i$ angles depend on $\theta_j^i$ angles through very simple relations (1), soon, we will no longer consider them.

$$\beta_3^i = -\theta_3^i; \quad \beta_2^i = \theta_2^i + \theta_1^i \tag{1}$$

In Figure 10 we can see how $\theta_2^i$ an $\theta_3^i$ spherical joint variables are depicted.

$\theta_2^i$ is the angle between the arm $A_iB_i$ and the plane called (Π) defined by the double parallel rods.

$\theta_3^i$ is the rotation angle of the double parallel rods in the (Π) plane.

It is important to focus on the fact that the spherical joints lead to mechanical limits on $\theta_3^i(\psi_3^i)$ given by relations (2):

$$|\theta_3^i| \leq \theta_{3\max}^i, i = 1, 2, 3 \quad |\psi_3^i| \leq \psi_{3\max}^i, \quad i = 1, 2, 3 \tag{2}$$

There is no limit on $\theta_2^i(\psi_2^i)$ but we consider them to be

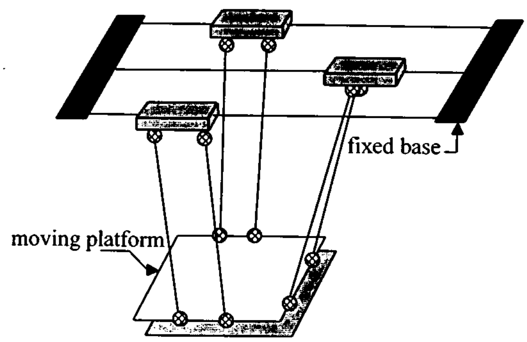


Fig. 2. H-Star robot.

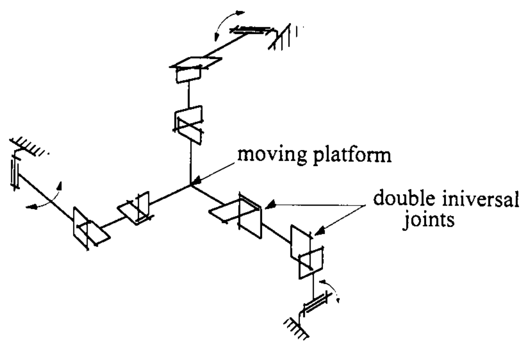


Fig. 3. Translation device with double universal joints.

https://doi.org/10.1017/S0263574797000507 Published online by Cambridge University Press

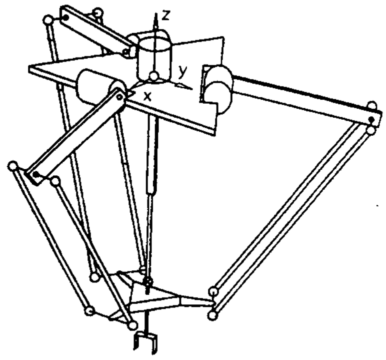


Fig. 4. Four d.o.f. Delta robot.

different from zero in order to avoid singular configurations.

$$\theta_2^i \neq 0, i = 1, 2, 3 \quad \psi_2^i \neq 0, \quad i = 1, 2, 3 \tag{3}$$

Finally, there are also mechanical limits on $\theta_1^i(\psi_1^i)$ so that:

$$\begin{aligned} \theta^i_{1\,\min} \leq \theta_1^i \leq \theta^i_{1\,\max}, \quad i = 1, 2, 3 \\ \psi^i_{1\,\min} \leq \psi_1^i \leq \psi^i_{1\,\max}, \quad i = 1, 2, 3 \end{aligned} \tag{4}$$

The end effector coordinates or task coordinates are:
—the position vector of the point $V$ referred to the fixed frame $R_0$. It is written as $OV^0 = (X_v, Y_v, Z_v)^T$, the index 0 recalls the reference frame.
—the Bryant angles $\gamma = (\gamma_1, \gamma_2, \gamma_3)^T$ of the frame $R_v$ attached to the end effector with respect to fixed frame.

The control variables are $\theta_1^i$ for $i$ equals 1 to 3 noted as $\theta_1$ vector $\theta_1 = (\theta_1^1, \theta_1^2, \theta_1^3)^T$. The three other active joint variables are the Bryant angles of the frame attached to the orientable base with respect to the fixed frame. These angles are written as $\phi = (\phi_1, \phi_2, \phi_3)^T$. Similar notations are used for passive joint variables as follows:

$$\theta_2 = (\theta_2^1, \theta_2^2, \theta_2^3)^T, \quad \theta_3 = (\theta_3^1, \theta_3^2, \theta_3^3)^T, \quad \psi_1 = (\psi_1^1, \psi_1^2, \psi_1^3)^T,$$
$$\psi_2 = (\psi_2^1, \psi_2^2, \psi_2^3)^T, \quad \psi_3 = (\psi_3^1, \psi_3^2, \psi_3^3)^T.$$

Due to the property of the Delta mechanism it is obvious that $\gamma$ equals $\phi$. Because of the mechanical limit of the spherical joint located at $D$, the angle between $Z_0$ and $Z_v$ axis is lower than $\alpha_{\max}$. Thus, the active joint variables $\phi_1$ and $\phi_2$ are subject to the following

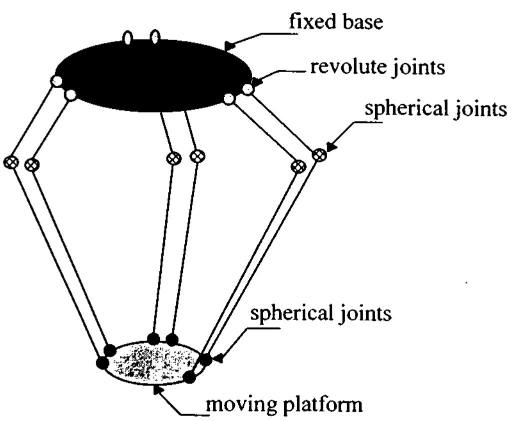


Fig. 5. The six d.o.f. Hexa robot.

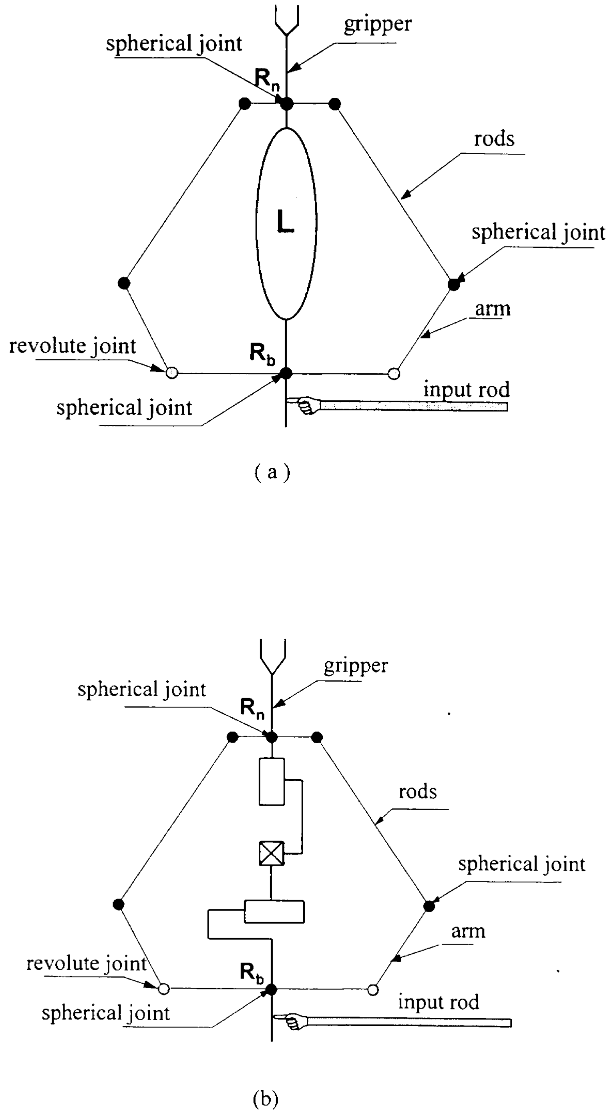


Fig. 6. Principle of uncoupling movement between orientation and translation of the gripper.

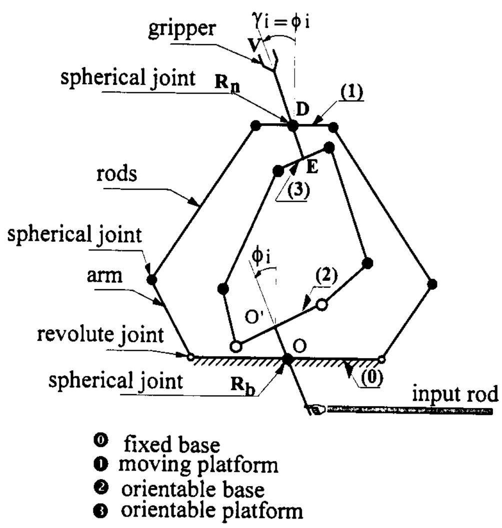


Fig. 7. The 6 d.o.f. 2-Delta robot.

https://doi.org/10.1017/S0263574797000507 Published online by Cambridge University Press

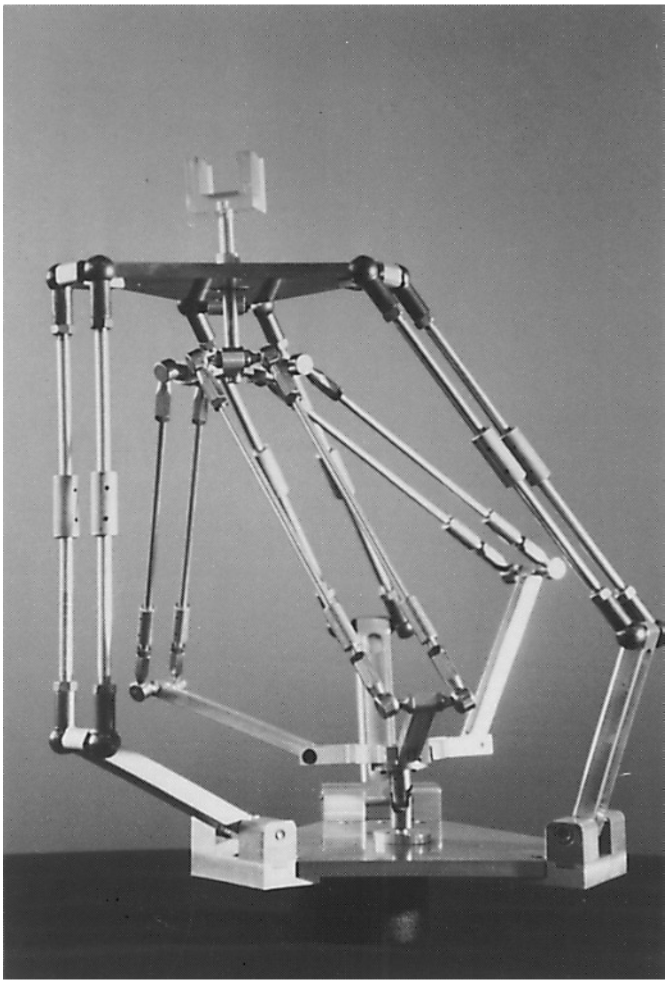

Fig. 8. Prototype of the 2-Delta architecture.

constraint:

$$\cos\phi_1 \cdot \cos\phi_2 \geq \cos\alpha_{max} \quad (5)$$

In order to obtain relationships between geometrical terms previously described we must use some results found by Clavel for the Delta architecture. Clavel gave closed-form relationships connecting cartesian coordinates of the point $D$ to the control variables $\theta_1$ and vice-versa. These relationships we will use are presented in the following way:

$$\text{Direct kinematics} \Rightarrow OD^0 = f(\theta_1) \quad (6)$$

$$\text{Inverse kinematics} \Rightarrow \theta_1 = f^{-1}(OD^0) \quad (7)$$

### *3.2 Solution to the direct kinematic problem for the 2-Delta robot*

The solution to the direct kinematic problem gives the position and the orientation of the gripper as well as passive joint variables of the external and the internal structure when control joint variables are known. Given terms are $\theta_1$ and $\phi$, unknowns are $OV^0$, $\gamma$, $\theta_2$, $\theta_3$, $\psi_1$, $\psi_2$, $\psi_3$.

Steps of the calculation are as follows:

—**Step 1.** The location of point $D$ is calculated by means of Clavel's relation (6)

—**Step 2.** Calculation of the location of point $V$ given by the following relation:

$$OV^0 = OD^0 + R(\phi)DV^{0'} \quad (8)$$

where $R(\phi)$ is the matrix transformation in Bryant angles from frame $R_{0'}$ with respect to frame $R_0$ and $DV^{0'} = (0, 0, DV)^T$.

—**Step 3.** Determination of the gripper orientation $\gamma$. It is obvious that:

$$\gamma = \phi \quad (9)$$

—**Step 4.** Calculation of passive joint variables $\theta_2$ and $\theta_3$ (external Delta).

Considering the kinematic chain numbered $i$, we write the vector $A_iC_i$ in two different ways:

$$A_iC_i^0 = A_iO^0 + OD^0 + DC_i^0 \quad (10)$$

$$A_iC_i^0 = R(Z_0, \alpha_i)R(Y_{Ai}, \theta_1^i) \times [A_iB_i^i + R(Y_i, \theta_2^i)R(Z_\pi, \theta_3^i)B_iC_i^{ri}] \quad (11)$$

Relation (10) involves points $A_i$, $O$, $D$ and $C_i$, in which each term is known. Relation (11) involves points $A_i$, $B_i$ and $C_i$ and rotation matrices between body frames depending on unknowns $\theta_2^i$ and $\theta_3^i$. These relations lead to both of the following equations

$$\sin\theta_3^i = k_1$$

$$\cos\theta_3^i(k_2\cos\theta_3^i + k_3\sin\theta_2^i) = k_4$$

whose solution results in $\theta_2^i$ and $\theta_3^i$. We complete this computation three times since $i$ equals 1 to 3.

—**Step 5.** Calculation of $\psi_1$ (internal Delta).

Firstly, we determine the position vector of point $E$ referred to the orientable base frame $R_{0'}$ by the following relation:

$$O'E^{0'} = O'O^{0'} + R^T(\phi)OD^0 + DE^{0'} \quad (13)$$

where $O'O^{0'} = (0, 0, -OO')^T$, $DE^{0'} = (0, 0, DE)^T$. Then, $\psi_1$ is a given according to Clavel's relation (7):

$$\psi_1 = f^{-1}(O'E^{0'}) \quad (14)$$

—**Step 6.** Calculation of $\psi_2$ and $\psi_3$ (internal Delta).

We use the same procedure as in step 4 after having expressed vector $H_iF_i$ referred to orientable base frame $R_{0'}$ instead of vector $A_iC_i$ referred to fixed base frame $R_0$.

### *3.3. Solution to the inverse kinematic problem for the 2-Delta robot*

In order to obtain the closed-form solution to the inverse kinematic we will use the following procedure.

Known terms are $OV^0$, the position vector point $V$, and the gripper orientation $\gamma$. Unknowns are the control joint variables $\theta_1$ and $\phi$, and the passive joint variables $\theta_2$, $\theta_3$, $\psi_1$, $\psi_2$, $\psi_3$.

—**Step 1** gives $\phi$ by

$$\phi = \gamma \quad (15)$$

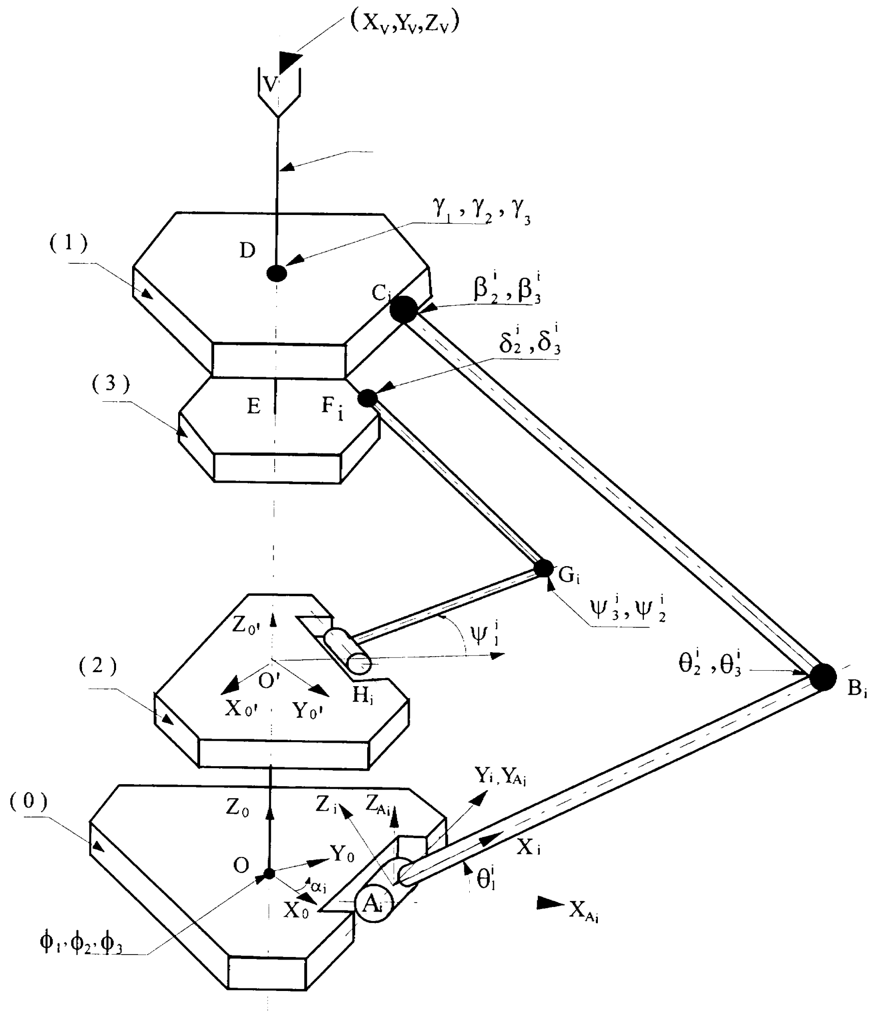


Fig. 9. Definition of joints parameters.

—**Step 2.** Calculation of position vector of point *D* referred to frame $R_0$:

$$OD^0 = OV^0 - R(\phi)DV^{0'} \tag{16}$$

where $R(\phi)$ and $DV^{0'}$ are previously defined.

—**Step 3.** Calculation of $\theta_1$ from the Clavel's relation (7).

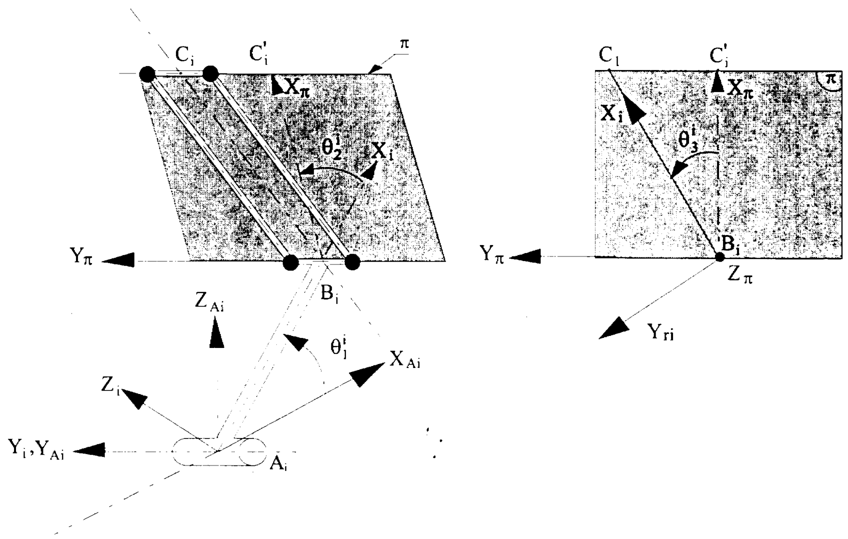


Fig. 10. Definition of angles $\theta_2^i$, $\theta_3^i$.

https://doi.org/10.1017/S0263574797000507 Published online by Cambridge University Press

Finally, the passive joint variables $\theta_2$, $\theta_3$, $\psi_1$, $\psi_2$, $\psi_3$ are obtained from the procedure (**steps 4, 5, 6**) described in the direct kinematic problem.

*3.4. "Checking" of the modeling*

Due to the complexity of kinematic modeling, many miscalculations were likely to appear. Thus it was necessary to check all the relationships. To this end, we built the 2-Delta architecture on a C.A.D. Robotic Simulator developed in our Laboratory[12] as it is shown in Figure 11. If the kinematic relationships are correct we will see that bodies remain connected together at joints when the mechanical structure is actuated. These figures allow us to check that the kinematic modeling is right.

## 4. GENERATION OF POSITION WORKSPACE AND ORIENTATION WORKSPACE

Starting from the knowledge of kinematic modeling we may obtain the workspace of the 2-Delta robot which depends on the mechanical limits of both active and passive joint variables.

To determine the position or the orientation workspace of the 2-Delta robot, we will use the technique of discretization[13] which consists, in this case, of the definition of the position workspace, of fixing the orientation of the end effector and finally seeking all positions that can be reached by the end effector, regardless of the cross section chosen. In the case of the generation of workspace orientation, we will consider the end effector position will be fixed. Then, we will seek all possible orientations. We have separated this space into two distinct subspaces:

Workspace without joint limits or theoretic space.
workspace with joint limits or space with constraints.

*4.1. Relationship between space of theoretical position and space with constraints*

The introduction of limits (relation (2) to (5)) on the passive and active joint variables reduces the workspace of the 2-Delta structure in comparison to the theoretical space. We have attempted to investigate the proportion that represents space with constraints in comparison to theoretical space. These two spaces in a cross section defined by plane $X_v = 0$ and plane $Z_v = 450$ mm are illustrated in Figure 12.

For a given cross section of the workspace (for example $Z_v$ = constant), we can evaluate the reachable surface by defining a workspace position factor $\delta_z$ as:

$$\delta_z = \frac{S_{p,c}}{S_{p,t}} \tag{17}$$

where, $S_{p,t}$ is the surface of theoretical space in the plane $Z_v$ = constant and $S_{p,c}$ is the surface of space with constraints in the same plane. It is obvious that $\delta_z$ depends on $Z_v$ and orientation $\gamma$. For example, in Figure 13, $\delta_z$ versus $Z_v$ for different orientations of the end effector are shown.

*4.2. Cross section of theoretical orientation space*

In order to obtain a representation in the plane, we will fix one of the three orientation angles of the gripper ($\gamma_3 = 0$), then will seek all possible orientations for a given position of point $V$ for both cases, without and with mechanical limits on joints. In Figure 14, (a) and (b) show two examples of two different cartesian coordinates of point $V$.

As we defined in (17) the position factor we could define the orientation factor $\eta_0$ as:

$$\eta_0 = \frac{S_{o,c}}{S_{o,t}} \tag{18}$$

where, $S_{o,t}$ is the surface of the theoretical orientation space and $S_{o,c}$ is the surface of the orientation space with constraints. It is obvious that $\eta_0$ depends on the position chosen for the point $V$. In Figure 15, $\eta_0$ versus $Z_v$ when the point $V$ belongs to $Z_0$ axis is shown.

## 5. MODELIZATION OF THE CLEARANCES IN POSITION AND IN ORIENTATION

In this section, we will consider the influence of the small variations of the rod lengths of the 2-Delta around their face values on translation and rotation vectors of the end effector. We will assume that these variations express the existence of localized clearance in the passive joints of the rods. Afterwards we will define the ellipsoïdes of clearance based on the concept of the manipulability ellipsoïds.[13]

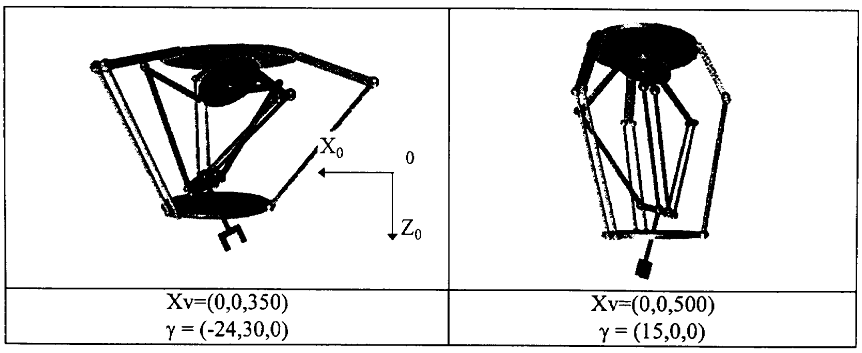


Fig. 11. Simulation of the 2-Delta robot.

https://doi.org/10.1017/S0263574797000507 Published online by Cambridge University Press

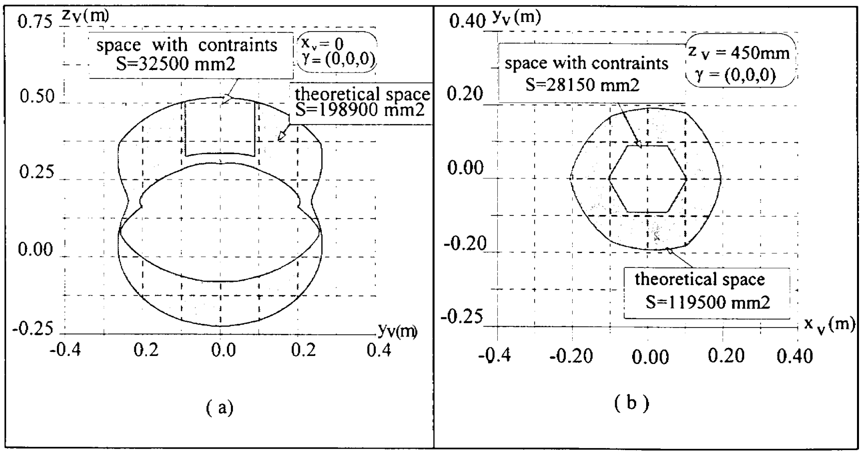


Fig. 12. Superposition of the theoretical space and the space with constraints (a) cross section for plane $X_V = 0$ (b) cross section for plane $Z_V = 450$ mm.

### *5.1. Problem statement and simplifying hypotheses*

In order to reduce the problem complexity, it seems useful to propose some simplifying hypotheses concerning the geometry of the robot, as well as its physical parameters. We suppose that:

–each parallelogram is made of one rod.

–all simulations are carried out taking into consideration that active joints are without clearances in each chosen configuration, and that the variation of the position and the orientation of the effector are due solely to variations of rod lengths which act as linear actuators.

We will separate the modelization of clearance into two parts:

–position clearance model which gives position variation of the effector solely for clearance at the passive joint of each rod of the external structure.

–orientation clearance model which gives orientation variation of the effector solely for clearance at the passive joint of the internal structure.

### *5.2. Position clearance model*

We define the position clearance model as,

$$\delta X_V = J_p \delta L_1 \qquad (19)$$

where:

$\delta X_v = (\delta x_V, \ \delta y_V, \ \delta z_V)^T$ represents the variations of the position of the end effector.

$\delta L_1 = (\delta L_1^1, \ \delta L_1^2, \ \delta L_1^3)^T$ represents the elementary length variations of the rods found in the external structure.

$J_p$ is the Jacobian matrix of partial derivatives of $X_V$ with respect to $L_1$, of dimension $3 \times 3$.

Terms of $J_p$ have complex expressions, thus we must

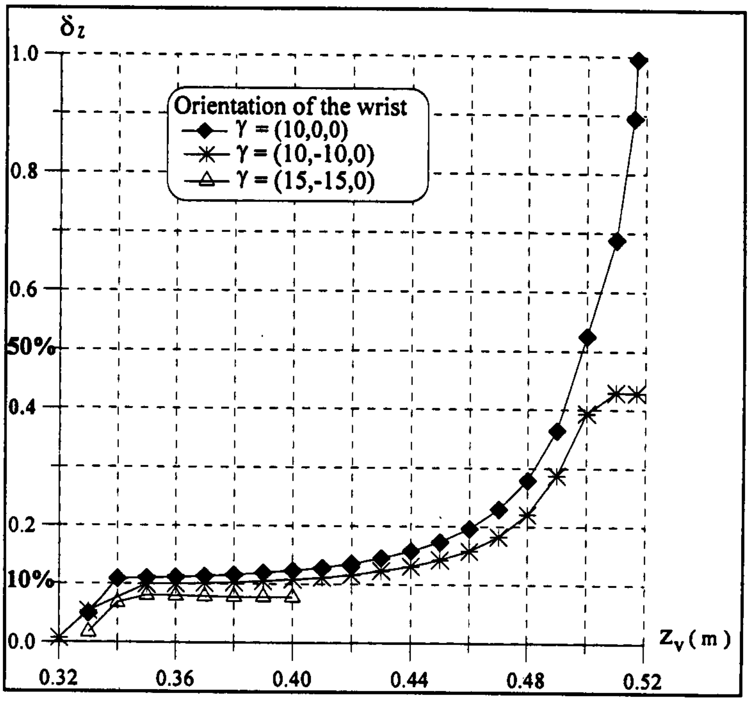


Fig. 13. Position factor on the axis $Z_0$.

https://doi.org/10.1017/S0263574797000507 Published online by Cambridge University Press

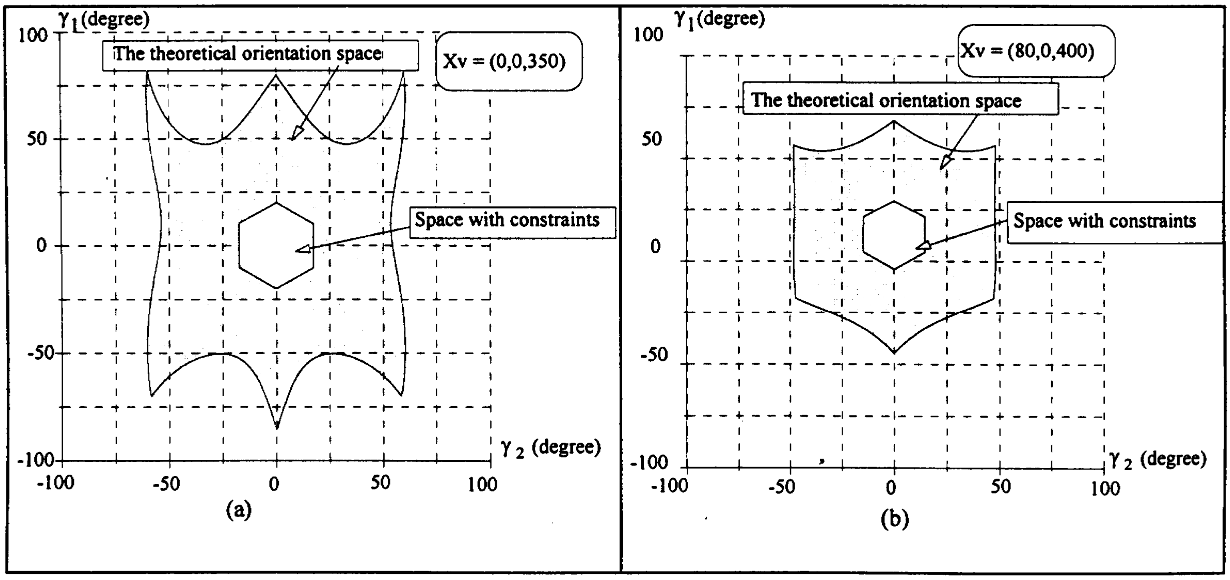


Fig. 14. Superposition of the orientation and with stops theoretical space for two sets of coordinates of point $V$.

use the symbolic calculation software (Maplle $V$) to obtain these expressions.

In Figure 16 there is a representation of the ellipsoid of clearance defined by $\delta X_v^T(JJ^T)^{-1}\delta X_v \leq 1$. When the effector moves along the $Z_0$ axis, we see that this axis constitutes an axis of revolution for these ellipsoïds the first two eigenvalues of each matrix $(JJ^T)^{-1}$ always remain equal ($\lambda_1 = \lambda_2$) whatever the position may be. This leads to an equitable distribution of the clearance in the plane $[x_0, y_0]$. Similarly, we observe that the volume of the ellipsoïds of clearance increases considerably as the position of the effector moves along the axis $z_0$. This is due to the vicinity of the singular configurations. On the other hand, for postures of the wrist following the axis $x_0$ or the axis $y_0$ (that is not shown here), the ellipsoids change in dimension and in form depending on their relation to the robot configuration. In fact, the clearance in these postures does not have the same effect in all directions.

The exploitation and the application of these results are very extensive. They allow, for example, a designer to know in advance the value of error in a position of the end effector according to the structure configuration. They also allow us to select the best configurations to execute a task inside the workspace.

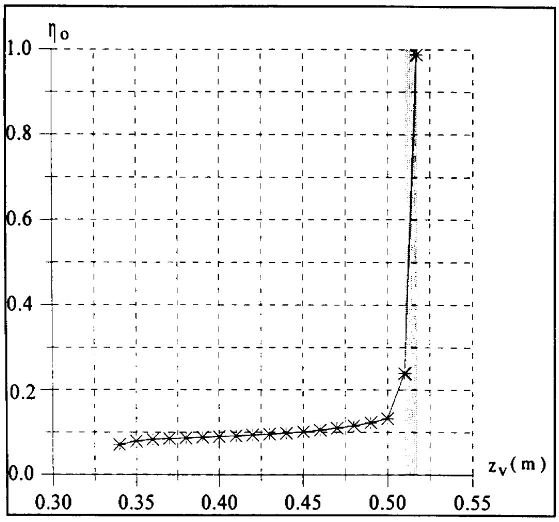


Fig. 15. Orientation factor on the axis $Z_0$.

### 5.3. *Orientation clearance model*

In this section, we will deal with the clearance at the passive joint of the internal structure on the gripper orientation. To obtain this model, we deduce it from the direct kinematic model which gives orientation coordinates of the gripper in relation to the rod lengths of the internal structure. Therefore we obtain:

$$\delta\gamma = J_0 \delta L_2 \tag{20}$$

where:

$\delta\gamma = (\delta\gamma_1, \delta\gamma_2)^T$ represents the variation of the orientation of the effector with $\gamma_3 = 0$.

$\delta L_2 = (\delta L_2^1, \ \delta L_2^2, \delta L_2^3)^T$ represents elementary length variations of the rod for internal Delta.

$J_0$ is the Jacobian matrix of partial derivatives of $\gamma$ with respect to $L_2$, of dimension $2 \times 3$.

We have studied ellipses of clearance in different positions. Presently, in Figure 17, we show the results of two ellipses obtained for two extreme positions on the axis $Z_0$.

We notice in general that eigenvalues which represent dimensions of clearance ellipse are roughly equal whatever the configuration. This shows that the uncertainty in orientation is almost the same in all postures (except postures close to single configuration). If we consider the obtained ellipses along the axis $z_0$ for orientation to be zero, we will observe that the surface of orientation uncertainty is represented by a circle since the two eigenvalues are equal, which shows that no direction is penalized. On the other hand, for configurations away from the axis $z_0$, we notice a dissymmetry represented by a change of ellipse

https://doi.org/10.1017/S0263574797000507 Published online by Cambridge University Press

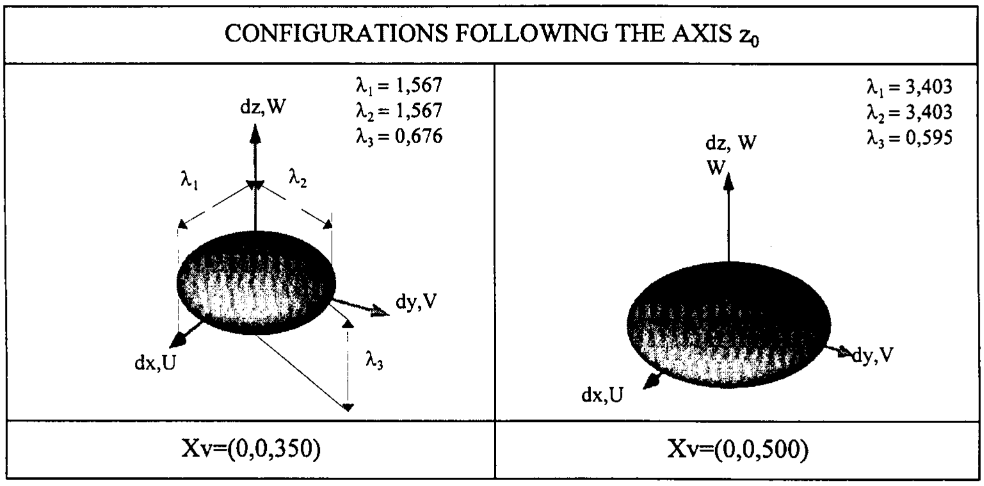


Fig. 16. Dimensions and morphology of the ellipsoids of position clearance on the axis $Z_0$.

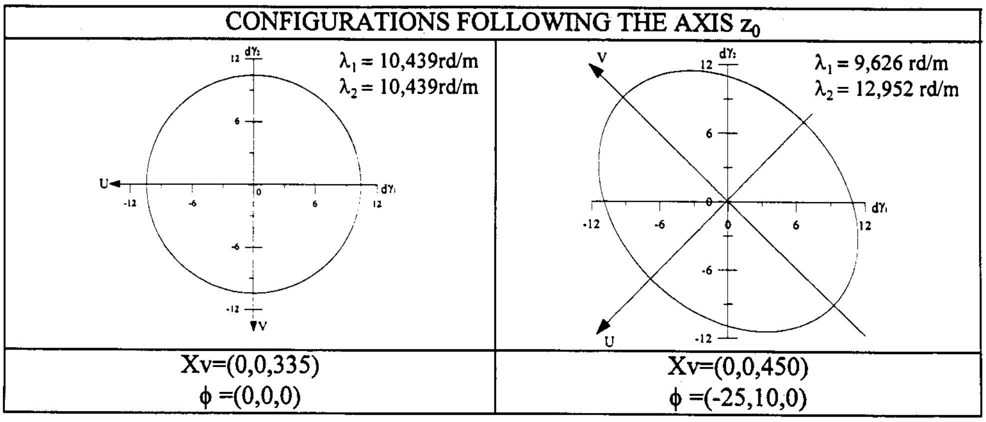


Fig. 17. Dimensions and morphology of clearance ellipses in orientation on the axis $Z_0$.

morphology, which explains the uncertainty difference due to the clearance that is not the same in all directions.

This study shows that the existence of passive joints, which in general characterize parallel robots, can be a source of error and perturbation and susceptible to producing position and orientation imprecisions of the effector. In the case of the 2-Delta robot, we have shown for distanced postures of singular configurations that the clearance has more influence on the position of the effector than on its orientation. In this section we have presented a methodology that allows one to identify and select configurations so that the effect of the clearance is minimized. Similarly the introduction of the ellipsoïdes of clearance (or ellipses of clearance) allows for a complete understanding of the general volume of the uncertainty in function of the configuration.

## 6. CONCLUSION

The main objective of this study consisted of examining a new parallel robot family, characterized by the uncoupled mechanics between the translation and rotation of the wrist, and proposing approaches to solve problems in design, modelization, joint limits and influence of the clearance. The study that we expect to do in the future will deal with the possible collisions between the internal and external Delta. With this aim in mind, we will use our CAD Robotic Simulator which contains a software especially designed for collision avoidance.

## References


1. W. Pollard and Evanston, "Position-Controlling Apparatus" *Application* April 22, 1938. Serial No. 203, 634 (Renewed June 14, 1940).
2. D. Stewart, "A Platform with six degrees of freedom" *IME Proc.* **80,** Part I (15) 371–386 (1965).
3. C. Reboulet, "Modélisation des robots parallèles" *Techniques de la Robotique* (Hermès, Paris, 1988) **Vol. 1,** pp. 257–284).
4. J.P. Merlet, "Commande par retour d'effort" *Thèse* (Université de Paris VI, 1986).
5. R. Clavel, "Une nouvelle structure de manipulateur parallèle pour la robotique légère" *RAIRO APII* **23,** No. 6, 501–519 (1989).
6. J.M. Herve and F. Sparacino, "Structural synthesis of parallel robot generating spatial translation" *ICAR 91,* Pisa, Italy pp. 808–813 (1991).
7. C. Reboulet, C. Lambert, N. Nombrail and N. Delpech, "Etude et mise en oeuvre du robot SPEED-R-MAN" *Rapport intermédiaire MRT/DERA* (December, 1991).
8. P. Jacquet, M. Dahan, G. Danescu and C. Garcin, "Robot parallèle à actionneurs linéaires *Le Congrès Français de Mécanique,* Lille, France (1991) pp. 377–380.


https://doi.org/10.1017/S0263574797000507 Published online by Cambridge University Press

9. A. Goudali, ''Contribution à l'Etude d'un Nouveau Robot Parallèle 2-Delta à Six Degrés de Liberté avec découplage'' *Thèse* (l'Université de Poitiers, 1995).
10. F. Pierrot, A. Fournier and P. Dauchez, ''Towards a fully parallel 6 d.o.f. robot for high speed, application'' *Proc. of the 1991 IEEE ICRA,* Saremento, California (April, 1991) pp. 1288–1293.
11. C. Gosselin and E. Lavoie, ''On the kinematic design of spherical 3-dof parallel manipulator'' *Int. J. Robotics Research* **12,** No. 4, 394–402 (1993).
12. S. Zeghloul, ''Développement d'un système de C.A.O.-Robotique intégrant la planification de tâches et la syntèse de sites robotisés'' *Thèse* de Doctorat d'Etat (Poitiers, 1991).
13. Y.C. Tsai and A.H. Soni, ''An algorithm for the Workspace of a General n-R Robot'' *ASME J. of Mechanisms, Transmissions an Automation in Design* **105,** No. 1, 52–57 (1983).
14. T. Yoshikawa, ''Manipulability of Robotic Mecanisms'' *Proceeding of the 2nd Int. Symposium on Robotic Research* (1984) pp. 439–446.